IOP PUBLISHING
IOP FTC
JOURNAL OF PHYSICS D: APPLIED PHYSICS
J. Phys. D: Appl. Phys. **41** (2008) 062004 (4pp)
doi:10.1088/0022-3727/41/6/062004

FAST TRACK COMMUNICATION

Ion energy and angular distributions into the wafer–focus ring gap in capacitively coupled discharges

Natalia Y Babaeva and Mark J Kushner[1]

Department of Electrical and Computer Engineering, Iowa State University, Ames, IA 50011, USA

E-mail: natalie5@iastate.edu and mjk@iastate.edu

Received 23 December 2007, in final form 8 February 2008
Published 21 February 2008
Online at stacks.iop.org/JPhysD/41/062004

Abstract
The termination of the edge of wafers in reactive ion etching reactors is important for obtaining uniform fluxes of reactants across the substrate. Structures such as focus rings (FRs) are often used to improve the uniformity of fluxes. There is a gap of hundreds of micrometres to a few mm between the edge of the wafer and the FR for mechanical clearance. Plasma penetration into the gap can produce particle forming films and erosion of consumable parts. In this paper, we discuss results from a computational investigation of ion energy and angular distributions incident into the wafer–focus ring gap. The geometry and electrical properties of the FR can skew the angle and limit the extent of energies of ions penetrating into the gap.

In plasma etching equipment for microelectronics fabrication, wafer terminating structures such as focus rings (FRs) are used to make the reactant fluxes uniform to the edge of the wafer, and so reduce the edge exclusion where useful products cannot be obtained. There is an engineered gap between the edge of the wafer and the FR, typically hundreds of μm to a few mm, to provide mechanical clearance. Plasma generated species can penetrate into this gap and under the bevelled edge of the wafer, depositing films and possibly creating particles. If the energy of the ions penetrating into the wafer–focus ring gap (WFG) are high enough and at critical angles, erosion of the substrate and FR may occur. The shape of the sheath over and in the gap can be influenced by the WFG geometry and the electrical properties (dielectric constant and conductivity) of the wafer and FR. This can in turn modify the orientation of electric fields and ion trajectories [1, 2]. In this regard, plasma moulding over steps, trenches and holes has recently been investigated [3, 4].

We previously showed that in radio frequency (rf) capacitively coupled plasmas (CCPs), the ratio of the Debye length (or sheath thickness) to the width of the WFG is an important parameter in determining plasma penetration [5]. Small ratios which result in the plasma being conformal in the WFG allow penetration of plasma species. In this paper, we discuss results from an extension of that study in which the ion energy and angular distributions (IEADs) into the WFG were computationally investigated in an rf CCP.

The plasma hydrodynamics portion of the model we used, *nonPDPSIM*, is essentially the same as that described in [5]. Briefly, the continuity equations for electron and ion densities, charge densities on and inside materials and Poisson's equation for the electric potential are simultaneously integrated using an implicit Newton's iteration technique. The fluxes of ions are computed by solving their momentum conservation equations. The electron temperature is obtained by integrating the electron energy conservation equation with transport coefficients derived from solving Boltzmann's equation. An electron Monte Carlo simulation tracks the trajectory of secondary electrons emitted from surfaces in regions of high electric field. Modified forms of the Navier–Stokes equations are solved for the neutral flow field. An unstructured mesh is used to resolve a dynamic range 100–1000 to

[1] Author to whom any correspondence should be addressed.

enable the reactor as well as the WFG to be accurately represented.

To compute IEADs to surfaces, a plasma chemistry Monte Carlo module (PCMCM), similar to that described in [6], was developed for *nonPDPSIM*. In the PCMCM, pseudoparticles representing ions and neutrals are launched from sites in the reactor with weightings proportional to their rate of generation by electron impact and heavy particle reactions. Monte Carlo techniques are used to advance their trajectories in time varying electric fields while accounting for elastic and inelastic collisions. The energy and angles of particles as they strike surfaces are recorded to provide a time averaged IEAD. Electric potentials as a function of rf phase computed on the unstructured mesh are interpolated onto a rectilinear structured mesh that overlays the unstructured mesh to enable the Monte Carlo algorithms to more rapidly execute. As particles move through the mesh, electric fields are interpolated in space and phase. Multiple nested structured meshes are used to resolve transport on the reactor scale as well as in the smaller features of the WFG. IEADs are collected as pseudoparticles strike surfaces and are recorded relative to the local normal.

A schematic of the CCP used in this investigation is shown in figure 1(*a*). A metal electrode is powered at 10 MHz and a 20 cm diameter Si wafer (conductivity $= 0.1\,\Omega^{-1}\,\mathrm{cm}^{-1}$, $\varepsilon/\varepsilon_0 = 8$) sits on the electrode. The wafer and electrode are surrounded by a FR (conductivity $= 10^{-8}\,\Omega^{-1}\,\mathrm{cm}^{-1}$, $\varepsilon/\varepsilon_0 = 4$). All other surfaces are grounded metal. Argon is injected through the shower head at 100 mTorr and 300 sccm, and exhausted through the pump port. The WFG in figure 1 is 1 mm wide (measured from the edge of the wafer) and the wafer edge is bevelled. The numbers on the wafer, electrode and FR in figure 1(*d*) indicate surfaces on which IEADs are collected. Regions 1–4 represent different surfaces on the wafer and have the same material properties. Region 5 is the metal substrate. Regions 6 and 7 are different surfaces of the FR and also have the same material properties.

The cycle averaged Ar^+ density for an applied voltage amplitude of 300 V is shown in figure 1(*b*) on the reactor scale and in figure 1(*c*) in the vicinity of the WFG. A peak plasma density of $1.2 \times 10^{10}\,\mathrm{cm}^{-3}$ diminishes to $4.5 \times 10^{8}\,\mathrm{cm}^{-3}$ at the top of the WFG. The Debye length at the top of the WFG is 700 μm, smaller than the gap size of 1 mm. As such, there is some plasma moulding into the gap.

The rf cycle averaged electric potential and IEADs incident on surfaces in and around a WFG of 500 μm are shown in figure 2 for FRs having $\varepsilon/\varepsilon_0 = 4$ and 20. (Although conventional materials for FR, such as alumina, have $\varepsilon/\varepsilon_0$ as large as 10, we chose $\varepsilon/\varepsilon_0 = 20$ for demonstration purposes.) The FR with $\varepsilon/\varepsilon_0 = 4$ has a smaller capacitance and charges more rapidly during the rf cycle. On a time averaged basis, this results in a larger potential drop inside the FR, which distorts the sheath and produces lateral electric fields in the WFG as shown in figure 2(*a*). The smaller capacitance of the FR results in ion fluxes into the gap being modulated during the rf cycle. A smaller potential drop inside the FR with $\varepsilon/\varepsilon_0 = 20$ leads to a more uniform sheath distribution over the WFG and ions penetrate into gap throughout the rf cycle (figure 2(*b*)). The wafer being more conductive sustains little voltage drop averaged over the rf cycle.

The cycle averaged IEADs for the FR having $\varepsilon/\varepsilon_0 = 4$ and 20 are compared in figures 2(*c*) and (*d*). The IEADs on the top surface of the wafer edge (surface 1) are nearly symmetric in angle. In spite of the dc bias being nearly the same in each case, the maximum energy of the IEAD is higher for $\varepsilon/\varepsilon_0 = 4$ due to the higher degree of modulation of the sheath in the vicinity of the FR. The bevel of the wafer (surface 2) has an angle of 19° to the horizontal. The average angle of incidence of the main portion of IEAD is 11° with a spread from 0° to 30°. This indicates that ions retain a significant portion of their vertically directed velocity resulting from acceleration in the unperturbed portion of the sheath above the WFG. However, they are redirected towards the local normal by the conformal nature of the sheath at the surface of the bevel during the anodic portion of the rf cycle. With $\varepsilon/\varepsilon_0 = 4$, the low energy portion of the IEAD arrives with nearly normal incidence, also due to the sheath being more conformal to the bevel during the anodic part of the cycle. The role of the inertia of ions is in large part determined by the proportion of the unperturbed sheath that is expended outside the gap. An ion whose velocity is largely a result of acceleration by the unperturbed sheath will likely not be significantly affected by the lateral fields within the gap.

For both $\varepsilon/\varepsilon_0 = 4$ and 20, the IEADs incident on the outer edge of the wafer (surface 3) have an angle of about 80° from the normal. In spite of ions being accelerated nearly vertically into the gap by the majority of the sheath residing outside the WFG, there are sufficient lateral electric fields in the gap to divert the ions from grazing incidence. Again, note that low energy ions strike the edge of the wafer with near normal incidence, due to the more conformal sheath during the anodic cycle. Similar trends are obtained for $\varepsilon/\varepsilon_0 = 20$ though the lower energy portion of the IEAD is less populated. The trends for the vertical surface of the FR (surface 6) are opposite to that of the wafer edge. The lower energy portion of the IEAD is less populated for $\varepsilon/\varepsilon_0 = 4$ as the lateral electric fields accelerate ions away from the FR surface.

The IEADs striking the horizontal substrate (surface 5) in the WFG have a narrower range of energy than striking the top of the wafer due to their fluxes being more modulated by the sheath in the gap. The IEAD for $\varepsilon/\varepsilon_0 = 20$ is nearly symmetric in angle whereas that for $\varepsilon/\varepsilon_0 = 4$ has a skew of about 10°, a consequence of the larger lateral electric fields in the WFG. The IEADs at the edge and on the top of the FR (surface 7) are nearly symmetric, and particularly so for $\varepsilon/\varepsilon_0 = 20$. The IEAD for $\varepsilon/\varepsilon_0 = 4$ again has a skew of about 5° resulting from the angled time averaged sheath near the edge of the FR.

Another design variable is the height of the FR. One extreme has the FR at the same level as the wafer and the other has the top of the FR 1 mm above the wafer. The time averaged electric potentials for $\varepsilon/\varepsilon_0 = 4$ are shown in figure 3(*a*) for the low FR and figure 3(*b*) for the high FR. With the low FR, the time averaged electric potential is skewed from the horizontal from a few millimetres interior to the edge of the wafer to many millimetres beyond the edge of the wafer. The low FR allows the sheath to be more conformal to the bevel whereas the high FR maintains a more horizontally oriented sheath with an angle to the bevel. As a result, the IEAD with the low FR on the top of the edge of the wafer (surface 1) is skewed 5°–10° from

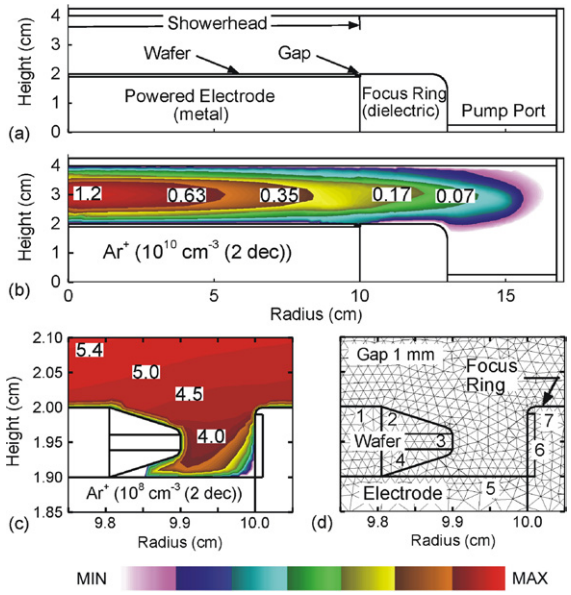

Figure 1. Schematic of the reactor with a 1 mm gap and time averaged plasma properties for argon (100 mTorr, 300 V, 10 MHz). (*a*) Full geometry. (*b*) Ar^+ density, (*c*) Ar^+ density in the gap and (*d*) close up of the WFG and unstructured mesh. Numbers on the wafer and FR indicate surfaces on which IEADs are computed.

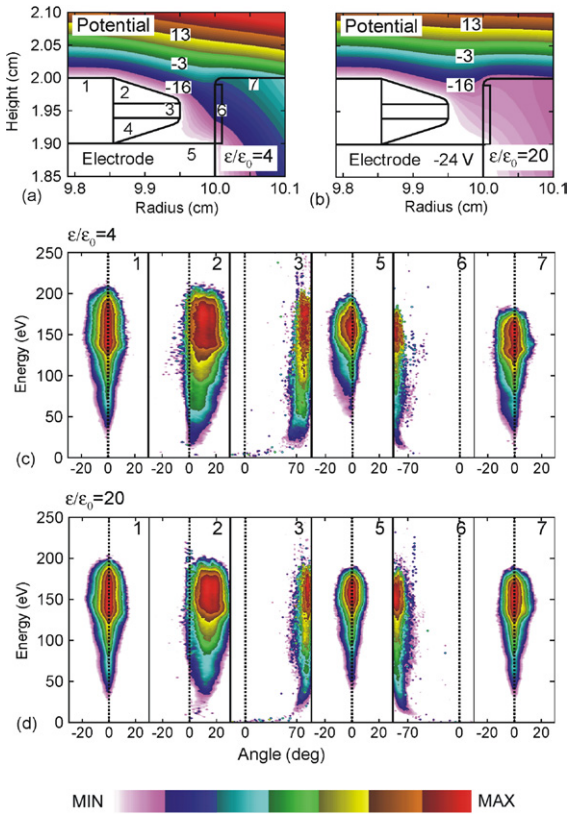

Figure 2. Plasma properties in the WFG with FRs having low and high capacitance for a 500 μm gap. Time averaged electric potential with (*a*) low ($\varepsilon/\varepsilon_0 = 4$) and (*b*) high capacitance ($\varepsilon/\varepsilon_0 = 20$). IEADs incident on different materials in the WFG with (*c*) low and (*d*) high capacitance. The numbers indicate the materials the ions strike. The IEAD contours span 3 decades on a log scale. IEADs for the high capacitance FR are more symmetric in angle and narrower in energy.

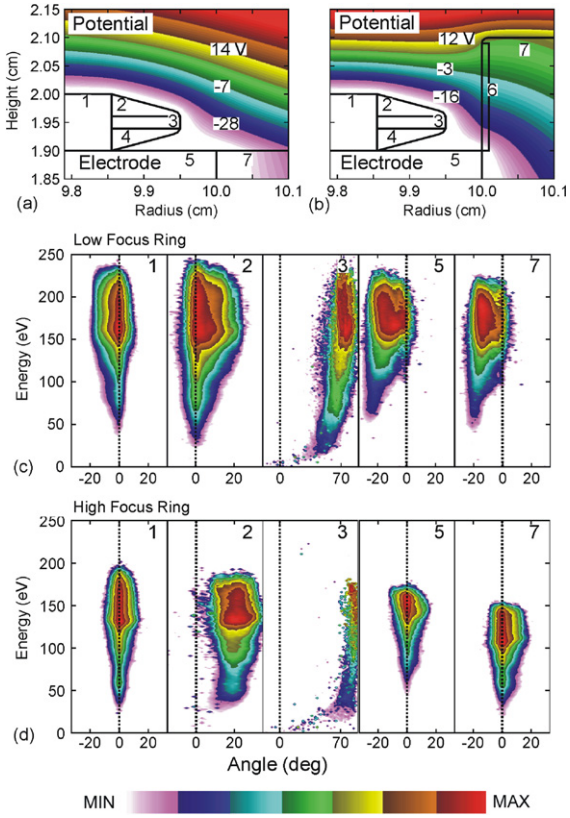

Figure 3. Plasma properties in the WFG with low and high FRs for a 500 μm gap. Time averaged electric potential with (*a*) low and (*b*) high FR. IEADs incident on different materials in the WFG with (*c*) low and (*d*) high FR. The numbers indicate the materials the ions strike. The IEAD contours span 3 decades on a log scale. The IEADS for the high FR are generally more symmetric.

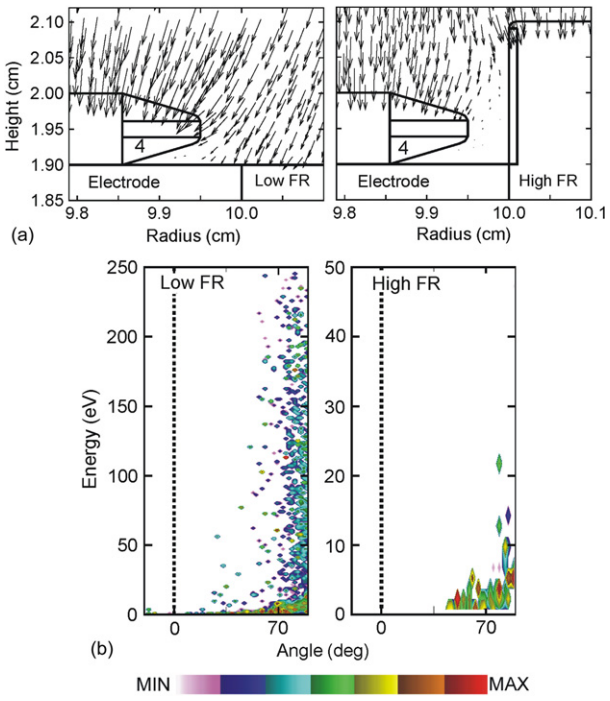

Figure 4. Plasma properties with FRs having low and high FRs. (*a*) Time averaged ion flux vectors for low and high FR. (*b*) IEADs incident on the underside of the bevel for low and high FR. The IEAD contours span 3 decades on a log scale.

the vertical, though extending to higher energies, whereas that for the high FR is nearly normal. The trend is opposite on the bevel (surface 2). With a more conformal sheath, the IEAD for the low FR has a broader range of energy and a more normal angle of incidence. With the high FR, the larger angle between the sheath and bevel produces an IEAD incident 20° from the normal with a narrower range of energies. Given that the bevel is offset by 19° from the horizontal, the ions are accelerated nearly vertically through the sheath.

The edge of the wafer (surface 3) with the low FR collects ion dominantly at 70° and extending to 225 V. Lower energy ions are collected progressively closer to the normal during the anodic part of the cycle. The skew in the sheath edge with the low FR produces an IEAD to the substrate (surface 5) that is nearly 20° from the normal whereas that with the high FR is centred about the normal. A similar trend occurs for the IEADs incident on the top of the edge of the FR (surface 7). Ion energies are lower by about 75 eV to surface 7 with the high FR due there being a voltage drop across the dielectric.

Due to their vertically oriented inertia from acceleration in the upper part of the sheath, few ions are incident on the underside of the bevel (surface 4), as shown by the time averaged ion flux vectors in figure 4 for low and high FR. There is some focusing of the ion flux at the outer vertex of the wafer with the low FR and at the top corner of the high FR. IEADs incident on the underside of the bevel are also shown in figure 4. With the low FR, ions are collected with energies extending to 225 eV during the cathodic part of the cycle at nearly grazing angles, though these ions are dominantly collected near the vertex. These ions arrive from larger radii with curved trajectories resulting from the curvature in the sheath edge (as shown in figure 3(*a*)). The ions collected on the deep underside of the bevel are at low energy after suffering scattering events. With the high FR, the high energy component of the IEAD is lost and ions are only collected at low energies after scattering events. Owing to the high FR, the high energy ions from large radii that contribute to the high energy tail with the low FR are blocked.

In conclusion, the IEADs incident into the WFG in CCPs were computationally investigated. The IEADs can be significantly skewed from the normal on the bevelled edge of the wafer and the substrate in the gap when the capacitance of the FR is such that time averaged lateral electric fields are produced. Low energy ions are more likely to arrive at normal incidence as the sheath is more conformal to the surface during the anodic part of the cycle. The height of the FR also has a significant effect on the skew of the IEADs. Designs which expose the edge of the wafer generally produce lateral electric fields and so skew the IEADs to off-normal angles.

Acknowledgments

This work was supported by Applied Materials Inc. and the Semiconductor Research Corporation.

References

[1] Czarnetzki U, Hebner G A, Luggenholscher D, Dobele H F and Riley M E 1999 *IEEE Trans. Plasma Sci.* **27** 70
[2] Jeon B, Chang H Y, Song J K and Jeon C W 2002 *Plasma Sources Sci. Technol.* **11** 520
[3] Kim D and Economou D J 2002 *IEEE Trans. Plasma Sci.* **30** 2048
[4] Kim D, Economou D J, Woodworth J R, Miller P A, Shul R J, Aragon B P, Hamilton T W and Willison C G 2003 *IEEE Trans. Plasma Sci.* **31** 691
[5] Babaeva N Y and Kushner M J 2007 *J. Appl. Phys.* **101** 113307
[6] Agarwal A and Mark J Kushner 2005 *J. Vac. Sci. Technol.* A **23** 1440